Arakawa, T., & Timasheff, S. N. (1984b) *Biochemistry 23*, 5924–5929.
Arakawa, T., & Timasheff, S. N. (1985) *Biochemistry 24*, 6756–6762.
Aune, K. C., & Timasheff, S. N. (1970) *Biochemistry 9*, 1481–1484.
Casassa, E. F., & Eisenberg, H. (1964) *Adv. Protein Chem. 19*, 287–395.
Cohn, E. J., & Ferry, J. D. (1943) in *Proteins, Amino Acids and Peptides* (Cohn, E. J., & Edsall, J. T., Eds.) pp 586–622, Reinhold, New York.
Edsall, J. T. (1943) in *Proteins, Amino Acids, and Peptides* (Cohn, E. J., & Edsall, J. T., Eds.) pp 140–154, Reinhold, New York.
Edsall, J. T., & Wyman, J. (1958) in *Biophysical Chemistry*, Academic, New York.
Ellerton, H. D., Reinfelds, G., Mulcahy, D. E., & Dunlop, P. J. (1964) *J. Phys. Chem. 68*, 398–402.
Ferry, J. D., & Oncley, J. L. (1941) *J. Am. Chem. Soc. 63*, 272–278.
Gekko, K., & Timasheff, S. N. (1981) *Biochemistry 20*, 4667–4676.
Inoue, H., & Timasheff, S. N. (1972) *Biopolymers 11*, 737–743.
Izumi, T., Yoshimura, Y., & Inoue, H. (1980) *Arch. Biochem. Biophys. 200*, 444–451.
Kirkwood, J. G. (1943) in *Proteins, Amino Acids and Peptides* (Cohn, E. J., & Edsall, J. T., Eds.) pp 276–303, Reinhold, New York.
Lee, J. C., & Timasheff, S. N. (1974) *Biochemistry 13*, 257–265.
Lee, J. C., & Lee, L. L. Y. (1979) *Biochemistry 18*, 5518–5526.
Lee, J. C., & Lee, L. L. Y. (1981) *J. Biol. Chem. 256*, 625–631.
Lee, J. C., & Timasheff, S. N. (1981) *J. Biol. Chem. 256*, 7193–7201.
Lee, J. C., Gekko, K., & Timasheff, S. N. (1979) *Methods Enzymol. 61*, 26–49.
Luzzati, V., Witz, J., & Nicolaieff, A. (1961) *J. Mol. Biol. 3*, 379–392.
Melander, W., & Horvath, C. (1977) *Arch. Biochem. Biophys. 183*, 200–215.
Nieuwenhuysen, P. (1979) *Biopolymers 18*, 277–284.
Noelken, M. E., & Timasheff, S. N. (1967) *J. Biol. Chem. 242*, 5080–5085.
Pappenheimer, J. R., Lepie, M. P., & Wyman, J., Jr. (1936) *J. Am. Chem. Soc. 58*, 1851–1855.
Pittz, E. P., & Timasheff, S. N. (1978) *Biochemistry 17*, 615–623.
Robinson, R. A., & Stokes, R. H. (1955) in *Electrolytic Solutions*, Butterworths, London.
Robinson, D. R., & Jencks, W. P. (1965) *J. Am. Chem. Soc. 87*, 2470–2479.
Roxby, R., & Tanford, C. (1971) *Biochemistry 10*, 3348–3352.
Timasheff, S. N., & Inoue, H. (1968) *Biochemistry 7*, 2501–2513.
Townend, R., Winterbottom, R. J., & Timasheff, S. N. (1960) *J. Am. Chem. Soc. 82*, 3161–3168.
von Hippel, P. H., & Schleich, T. (1969) in *Structure and Stability of Biological Macromolecules* (Timasheff, S. N., & Fasman, G. D., Eds.) pp 417–574, Marcel Dekker, New York.
Wyman, J. (1964) *Adv. Protein Chem. 19*, 223–286.

Trypsinogen–Trypsin Transition: A Molecular Dynamics Study of Induced Conformational Change in the Activation Domain†

Axel T. Brünger,‡,‖ Robert Huber,§ and Martin Karplus*,‡
Department of Chemistry, Harvard University, Cambridge, Massachusetts 02138, and Max-Planck-Institut für Biochemie, D-8033 Martinsried bei München, FRG

Received July 1, 1986; Revised Manuscript Received May 8, 1987

ABSTRACT: The trypsinogen to trypsin transition has been investigated by a stochastic boundary molecular dynamics simulation that included a major portion of the trypsin molecule and the surrounding solvent. Attention focused on the "activation domain", which crystallographic studies have shown to be ordered in trypsin and disordered in its zymogen, trypsinogen. The chain segments that form the activation domain were found to exhibit large fluctuations during the simulation of trypsin. To model a difference between trypsin and trypsinogen, the N-terminal residues Ile-16 and Val-17 were removed in the former and replaced by water molecules. As a result of the perturbation, a structural drift of 1–2 Å occurred that is limited to the activation domain. Glycine residues are found to act as hinges for the displaced chain segments.

Trypsin is an enzyme for which the functional significance of flexibility has been established. It is known that activation of the zymogen, trypsinogen, by removal of the N-terminal hexapeptide is directly coupled to a flexible to rigid transition in a relatively localized region of the trypsin molecule (Huber & Bennett, 1983; Bennett & Huber, 1985). X-ray structures of trypsin, trypsinogen, and a number of inhibitor-bound complexes solved at high resolution (Huber & Bode, 1978; Kossiakoff et al., 1977) provide information concerning the transition. Also, equilibrium and kinetic data are available (Keil, 1971; Bode & Huber, 1976). However, the detailed dynamics of the transition, including the essential interactions

† This work was supported by the National Science Foundation (A.T.B. and M.K.) and the Max-Planck-Institut für Biochemie (A.T.B. and R.H.). The CRAY time was supplied by a grant from the Office of Advanced Scientific Computing of the National Science Foundation.
‡ Harvard University.
‖ Present address: Howard Hughes Medical Institute and Department of Molecular Biology, Yale University, New Haven, CT 06511.
§ Max-Planck-Institüt für Biochemie.

0006-2960/87/0426-5153$01.50/0

involved, have not been determined. It is for this reason that molecular dynamics simulations (McCammon & Karplus, 1983) aimed at elucidating the processes involved in the activation of trypsin have been undertaken. This paper reports the initial results of such a study.

Trypsin exists in two different states: the catalytically inactive proenzyme trypsinogen and the active trypsin molecule. Trypsinogen is converted to trypsin by cleavage of the N-terminal hexapeptide. The two molecules have essentially identical structures for about 85% of the chain; the deviation of the main-chain atoms in this part of the molecule is only 0.2 Å (Huber & Bode, 1978). The remaining 15% of the molecule forms the so-called "activation domain" (Huber & Bode, 1978). It is partly or entirely disordered in trypsinogen at physiological temperatures (Bode et al., 1976; Fehlhammer et al., 1977; Kossiakoff et al., 1977) as well as at low temperatures (Walter et al., 1982). In the trypsin molecule, where the N-terminal residue is Ile-16 (chymotrypsin notation), the activation domain is well ordered. It consists of three loop segments (Gly-142 through Pro-152, Gly-154 through Gly-193, and Gly-216 through Thr-222) and the N-terminal sequence Ile-16, Val-17, Gly-18, which is bound to a binding pocket formed by the activation domain. The salt link between Ile-16 and Asp-194, which is adjacent to a segment of the activation domain, seems to be necessary to trigger the transition from trypsinogen to trypsin (Huber & Bode, 1978); i.e., any discharge, removal, or blocking of the Ile-16 amino group in the homologous enzyme chymotrypsin leads to inactivation (Sigler et al., 1968). Among other enzyme/zymogen systems, the chymotrypsinogen/chymotrypsin system (Blow, 1976; Cohen et al., 1981; Wang et al., 1985) and the α-phospholipase system (Matthews & Hudson, 1986) have features similar to those of trypsin. In particular, parts of the activation domain in chymotrypsinogen are disordered or differ in structure among molecules with different crystal contacts (Wang et al., 1985).

It has been suggested that trypsinogen represents an incompletely folded trypsin species with structural variability and deformability in the activation domain (Huber & Bode, 1978). The correct folding of the activation domain is achieved in trypsin (i.e., when the N-terminal hexapeptide has been cleaved) and in trypsinogen in the presence of a strongly bound ligand (e.g., the bovine pancreatic trypsin inhibitor) and a dipeptide, such as Ile-Val or Val-Val, that is similar to the N-terminus of trypsin (Bode & Huber, 1976). The contact areas of substrates involve parts of the activation domain, as can be inferred from the crystal structure of the trypsin–PTI complex (Huber et al., 1974).

Thus, substrate binding is expected to be affected by the flexibility of the activation domain in trypsinogen. The structure of the trypsinogen–PTI complex (Bode et al., 1976) is very similar to the trypsin–PTI complex, with the exception of the autolysis loop (residues Gly-142 to Pro-152), which is only partly ordered, and the N-terminus, which remains invisible up to residue 18 and is probably disordered in solution.

Perturbed angular correlation measurements on mercury labels (Butz et al., 1982) suggest that there exists a dynamical relaxation process in the nanosecond time regime ($\sim$10 ns) in the activation domain in trypsinogen; no such process is observed in the trypsin-like structure of the trypsinogen–PTI complex. This time constant is of the order of diffusional relaxation found in polypeptides by stochastic dynamics simulations (McCammon et al., 1980). Since conventional molecular dynamics simulations for large macromolecular systems are generally limited to subnanosecond periods, it is difficult to examine the relaxation process directly. It should be noted, however, that the greater speed and availability of supercomputers will make possible simulations in the nanosecond time regime in the near future.

Before undertaking such large-scale simulations it is essential to have some insight into the nature of the process involved. As a first step in such an analysis, we use molecular dynamics in the present work to sample the conformational space of the trypsin molecule in the neighborhood of its native (equilibrium) conformation. Similar conformational regions are expected to be involved in both equilibrium fluctuations and transitions between two states of the molecule, if they are sufficiently close (Ansari et al., 1985). We then perturb an equilibrated trypsin molecule and use molecular dynamics to characterize the conformational change. We investigate the transition from trypsin to trypsinogen, rather than the reverse, because only trypsin has a well-ordered structure that is a convenient starting point for the simulation. The perturbation mimics the change to trypsinogen by removing the two N-terminal residues (Ile-16, Val-17) of trypsin and replacing them by water molecules. The starting structure Tr(−16,17)MD[1] is a model for that observed in the trypsinogen–PTI complex, where the binding pocket is filled with water molecules and the N-terminus is disordered. Such a structure, in the absence of the PTI inhibitor, has been postulated as an intermediate along the pathway of the transition between trypsinogen and trypsin (Huber & Bode, 1978).

In the present study, the effect of the perturbation is examined on a picosecond time scale. Ideally, one would carry out a simulation of Tr(−16,17)MD to the nanosecond time regime and beyond. The molecule would then "relax" to a trypsinogen-like conformation with a disordered activation domain or it would stay "trapped" in a trypsin-like conformation. The former outcome would provide support for the idea that the binding of the N-terminus in trypsin is the triggering event for the "rigidification" of the activation domain; the latter outcome would suggest a more complicated reaction scheme for the trypsinogen–trypsin transition. This question will be subject of future theoretical investigations by special simulation methods (e.g., activated and stochastic dynamics; McCammon & Karplus, 1983).

Because the region of primary interest in the present study is on the surface of the molecule, solvent effects are expected to be important. Consequently, a vacuum simulation of the type frequently used to study the dynamics of macromolecules would not be adequate. To treat the solvated system, we use the stochastic boundary molecular dynamics (SBMD) methodology (Brünger et al., 1984, 1985; Brooks et al., 1985a); it is summarized under Methods. The SBMD method was introduced to simulate a relatively small region such as the active site of the molecule and its immediate surroundings (Brünger et al., 1985). Here we report the application of the SBMD method to a large system that consists of about 90% of the trypsin molecule plus several solvation layers surrounding most of the molecule. The SBMD method is more efficient than a conventional periodic boundary molecular dynamics simulation for solvated trypsin; i.e., the number of water molecules included here is 668 in contrast to the 4785 used recently in a full simulation of the trypsin–benzamidene complex (Wang & McCammon, 1986). Under Results we characterize the

[1] Abbreviations: SBMD, stochastic boundary molecular dynamics; TrMD1, SBMD simulation of trypsin, 10–20 ps; TrMD2, continuation of TrMD1, 20–30 ps; Tr(−16,17)MD, SBMD simulation of trypsin without Ile-16 and Val-17 residues; (16,17)MD, SBMD simulation of the isolated Ile-16 and Val-17 dipeptide.

properties of the average molecular dynamics structure and compare them with the X-ray data on trypsin. We then analyze the conformational changes occurring in the perturbed trypsin system with the Ile-16 and Val-17 residues replaced by water.

METHODS

Energy Calculations. Empirical potential energy functions for the molecular dynamics calculations were taken from Brooks et al. (1983), in which nonpolar groups are represented by an extended atom model and polar hydrogens are treated explicitly. The hydrogen-bonding potential used by Brooks et al. (1983) was replaced by the appropriate parameterization of the Lennard–Jones and electrostatic nonbonding energy terms (CHARMM, version 19). Solvent molecules were treated by the TIP3P model (Jorgensen et al., 1983) with protein–solvent and protein–protein hydrogen-bonding parameters adjusted to yield consistent values for the well depths (W. Reiher and M. Karplus, unpublished results). The Lennard–Jones interactions were multiplied by a cubic switching function (Brooks et al., 1983), and the electrostatic interactions were multiplied by the quartic shifting function $1 - 2(r/c)^2 + (r/c)^4$ (Brooks et al., 1985b); interactions were included up to 8.5 Å. A dielectric constant of unity was employed throughout the system.

Integration of the equations of motions was performed by use of a Verlet integrator algorithm (Verlet, 1967), modified for the integration of simple Langevin equations (Brünger et al., 1984), with initial velocities assigned from a Maxwellian distribution at 300 K. Bond lengths involving hydrogen atoms in the protein and both bond lengths and bond angles in water molecules were kept fixed with the SHAKE algorithm (Ryckaert et al., 1977). The time step of the integrator was 1 fs, and the nonbonded list was updated every 20 fs.

Computations were performed on a CRAY-1S computer with 8 Mbyte of memory (University of Minnesota Computing Center) using the program CHARMM (Brooks et al., 1983), version 19, optimized for the CRAY. The total CPU time necessary for this work was about 40 h. The structures were displayed on an Evans and Sutherland PS300 with a modified version of the function network of FRODO (Jones, 1982; Pflugrath et al., 1984) interfaced with CHARMM.

Stochastic Boundary Molecular Dynamics. The X-ray structure of trypsin solved and refined at 1.8-Å resolution by Bode and Schwager (1975) was used as a starting point for all the simulations. This structure provided coordinates for 1629 protein heavy atoms and the oxygen positions of 88 ordered water molecules.

The stochastic boundary molecular dynamics method partitions the system into three regions: the *reaction region* consisting of the region of interest (in this case the activation domain and its surroundings; see Figure 1); the *buffer region* that surrounds the reaction region; and the *excluded region* consisting of the remainder of the system. The reference point for the partitioning was chosen halfway between residue Ile-16 and the catalytic residue His-57 in the X-ray structure. This reference point minimizes the radius of a sphere required to include the activation domain, the active site of trypsin, and a significant part of the rest of the protein. A radius of 22 Å was used. This is large enough to ensure that not only the activation domain but also the surroundings are completely solvated (Figure 2). To obtain the initial positions of the water molecules, a sphere of water molecules was centered at the reference point and any water with the center of its oxygen within 2.6 Å of a heavy protein atom or an ordered water oxygen atom from the crystal structure was deleted. The water

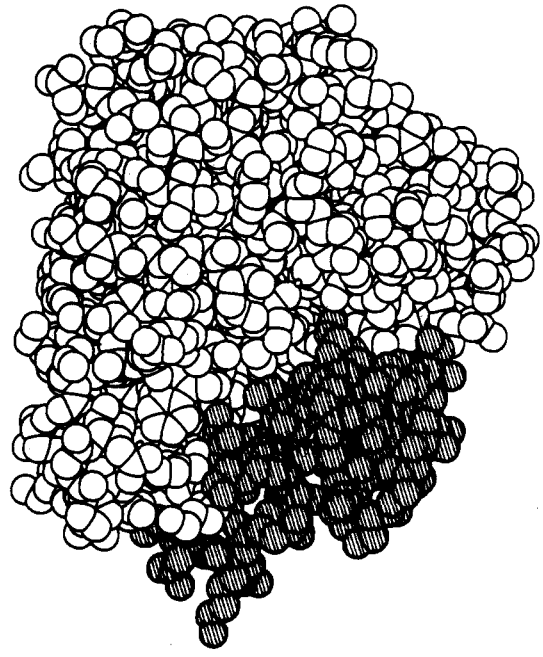

FIGURE 1: Space-filling drawing of trypsin. The shaded area indicates the activation domain.

positions in the sphere were taken from a previously equilibrated Monte Carlo simulation of TIP3P waters (Jorgensen et al., 1983). The resulting structure is illustrated in Figure 2.

Atoms were labeled as excluded region atoms if they were part of a residue for which all mainchain (N, C^{α}, and C) and side-chain atoms were outside the 22-Å radius measured from the reference point. All side-chain atoms of a particular residue were labeled as reaction region atoms if any side-chain atom was less than 20 Å from the reference point. The partitioning of main-chain atoms between reaction and buffer regions was carried out on a strict spherical criterion: any main-chain atom within a 20-Å radius of the reference point was labeled as a reaction region atom. The remaining atoms, those roughly between 20.0 and 22 Å, were labeled as buffer region atoms. Protein atoms were assigned to a given region for the entire simulation; water molecules were allowed to diffuse freely between the buffer region and the reaction region. The resulting system (Figure 2) contained 1626 protein atoms in the reaction region, 195 protein atoms in the buffer region, and 668 water molecules (after equilibration, see below) in the two regions combined.

Atoms in the excluded regions were neglected, atoms in the buffer region were propagated as Langevin particles with appropriate boundary forces, and atoms in the reaction region were treated as "normal" molecular dynamics atoms (Brünger et al., 1984; Brooks et al., 1985a).

Boundary forces for the water molecules were derived from an effective boundary potential on the water oxygen atoms; the effective boundary potential for TIP3P water was obtained in a way similar to the one for ST2 water described in Brünger et al. (1984). This boundary force field prevents the otherwise unconstrained water molecules from escaping. The friction coefficient for water oxygen atoms in the buffer region was set equal to 62 ps^{-1} which corresponds to the self-diffusion constant of water at 300 K. The reaction vs. buffer region labeling for water molecules was updated every 5 fs.

Boundary forces for the protein buffer region atoms were represented as harmonic restoring forces (Brooks et al., 1985a) with force constants derived from the atomic mean-square fluctuations of trypsin, which were approximated by the trypsin

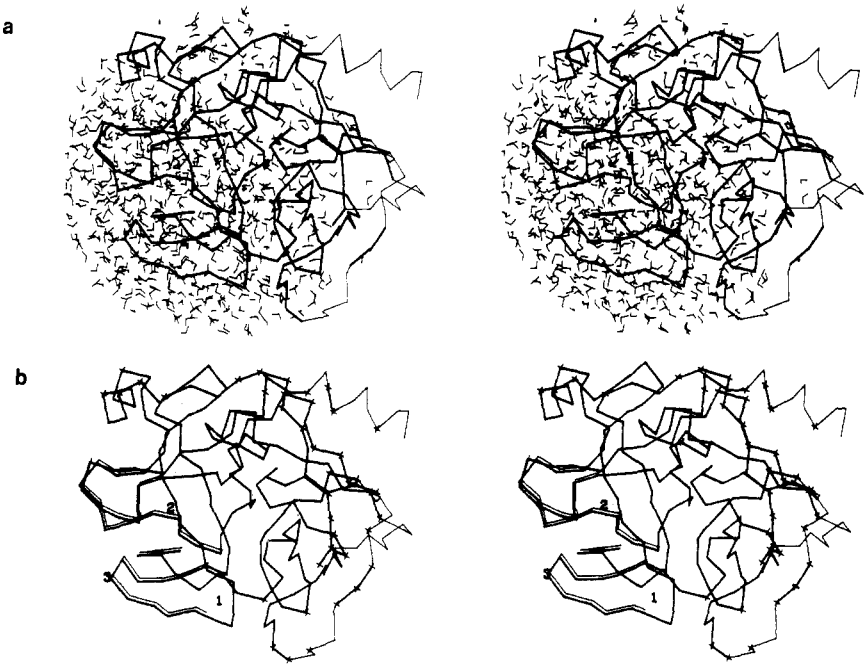

FIGURE 2: Solvated trypsin molecule within stochastic boundary. The C^{α} backbone of the protein is shown, where the thin lines indicate regions that have been eliminated in the SBMD simulation (excluded region, see text) and the thick lines correspond to the reaction region. In (a) the atoms of water molecules are superimposed on the C^{α} backbone. In (b) the constrained buffer region residues are marked by a + and the activation domain is indicated by double lines. Three points (1–3) are marked where the water density was measured during the simulation.

X-ray temperature factors averaged over classes of atoms (main chain without O, B = 13.97; main-chain O, B = 13.95; β-side-chain atoms, B = 13.86; γ-side-chain atoms, B = 15.93; δ-side-chain and all remaining side-chain atoms, B = 16.17). The friction coefficient was set to 200 ps^{-1} for all protein buffer region atoms (Brooks et al., 1985a). An interatomic screening function $S(r)$ was applied to the harmonic force constants and to the friction coefficients for protein atoms in the buffer region

$$S(r) = \frac{(r - R_B)^2(3R_E - R_B - 2r)}{2(R_E - R_B)^3} \qquad (1)$$

where r is the distance to the center of the reaction region, R_B = 20 Å is the reaction/buffer region boundary, and R_E = 22 Å is the buffer/excluded region boundary. The function $S(r)$ is zero at R_B and 0.5 at R_E. Such a screening function is introduced to account for the fact that buffer region atoms close to the reaction/buffer boundary interact on the average with more atoms than atoms closer to the excluded region. Therefore, atoms close to the excluded region should feel a larger harmonic force and friction coefficient to approximate the missing interactions. The introduction of the screening function represents an improvement of the method described in Brooks et al. (1985a); in particular, dynamical properties, such as displacement autocorrelation functions, show better agreement with calculations on the full system (unpublished results).

Computational Strategy. Hydrogen positions were constructed for the initial SBMD structure (Figure 2) consisting of 1821 protein atoms, the Ca^{2+} ion, and 580 water molecules (Brünger & Karplus, 1987), and the structure was subjected to 200 cycles of conjugent gradient energy minimization (Powell, 1977) with harmonic constraints applied uniformly to all atoms with an initial force constant of 40 kcal/(mol Å^2) decreasing to 10 kcal/(mol Å^2) in decrements of 1.5 kcal/mol every 20 steps (Bruccoleri & Karplus, 1986). This was followed by 8 ps of SBMD dynamics at 300 K with all protein degrees of freedom fixed. Another 8 ps of SBMD dynamics was carried out where all protein and water molecules were allowed to move. A new 22.0-Å sphere of water molecules was centered at the reference point, and any water molecule that overlapped with a heavy protein atom or any water molecule from the previous simulation was deleted. This procedure added 88 new water molecules to the system. Another 10 ps of SBMD dynamics with all protein and water atoms free to move followed. This completed the setup, equilibration, and thermalization of the system which now consisted of 3826 atoms, including 668 water molecules.

The next 10 ps of SBMD dynamics was used for analysis and will be referred to as TrMD1 in the following. As a test for the quality of the water equilibration in the TrMD1 run the water density was computed at three different points. The values were 0.0346, 0.0351, and 0.0364 mol/Å^3 for the points labeled 1–3 in Figure 2b, respectively, in satisfactory agreement with the mean density of water (0.03332 mol/Å^3) at 300 K (1 atm). The position of the first maximum of the g_{00} radial distribution function is at 2.8 Å, in good agreement with pure water simulations (Brünger et al., 1984).

To test its convergence properties and as a control for the perturbed trypsin calculation, the TrMD1 simulation was continued for additional 10 ps. This will be referred to as TrMD2.

Replacement of the Ile-16 and Val-17 Residues by Water Molecules. The final coordinate set of the molecular dynamics run TrMD1 was taken as the starting point for the perturbation calculation. Residues Ile-16 and Val-17 were deleted; the charges on Asp-194 and Gly-18 were left unaltered. With the overlay procedure described in the previous section, it was determined that five water molecules were required to fill the void left by the missing two residues. A 10-ps period of SBMD dynamics was carried out with the five new water molecules, and all other water and protein atoms free to move. During this time two additional water molecules diffused from the immediate vicinity of the activation domain into the binding pocket; one water molecule was already present in the binding pocket in TrMD1. Finally, 10 ps of SBMD dynamics was carried out; this period was used for analysis and is referred to as the Tr(−16,17)MD simulation.

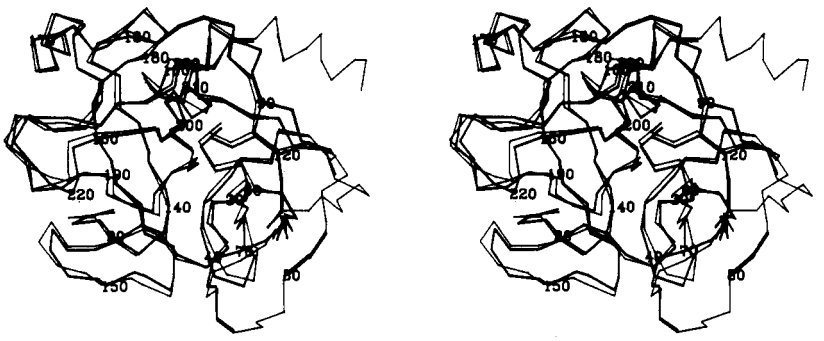

FIGURE 3: Comparison of the C^{α} backbone of the X-ray structure of trypsin (thin lines) and the average molecular dynamics structure of the TrMD1 run (thick lines).

Table I: Secondary Structure of Trypsin

classification	ident[a]	residue range
activation domain[b]	1	Ile-16 to Gly-19
	2	Gly-142 to Pro-152
	3	Gly-184A to Gly-193
	4	Gly-216 to Asn-223
β-sheet[c]	5	Tyr-20, Lys-156 to Pro-161, Cys-136 to Gly-140, Gly-197 to Cys-201, Lys-204 to Ser-214, Gly-226 to Val-231, Asn-179 to Ala-183
β-sheet[c]	6	Gly-43 to Ser-45, Val-52 to Ala-55, Met-104 to Lys-107, Lys-87 to Val-91
β-sheet[c]	7	Ile-63 to Arg-66, Gln-81 to Ala-85
α-helix[c]	8	Ser-164 to Tyr-172
α-helix[c]	9	Lys-230 to Asn-245
β-turn[d]	a	Asn-25 to Pro-28
	b	Asn-34 to Tyr-39
	c	Asn-48 to Trp-51
	d	Ala-55 to Cys-58
	e	Asn-72 to Val-75
	f	His-91 to Tyr-94
	g	Ser-96 to Leu-99
	h	Asn-115 to Val-118
	i	Ser-130 to Thr-134
	j	Lys-145 to Gly-148
	k	Tyr-172 to Gln-175
	l	Thr-177 to Met-180
	m	Tyr-184 to Gly-187
	n	Cys-191 to Asp-194
	o	Asp-194 to Gly-197
	p	Cys-201 to Lys-204
	q	Ala-221A to Lys-224

[a] Identification used throughout this paper. [b] Definition of the activation domain according to Huber and Bode (1978). [c] Definition of secondary structure according to Chambers and Stroud (1977). [d] Turns defined as consecutive residues (i, ..., $i + 3$) where the separation between C^{α} (i) and C^{α} ($i + 3$) is less than 6.0 Å. This definition taken from Chou and Fasman (1978).

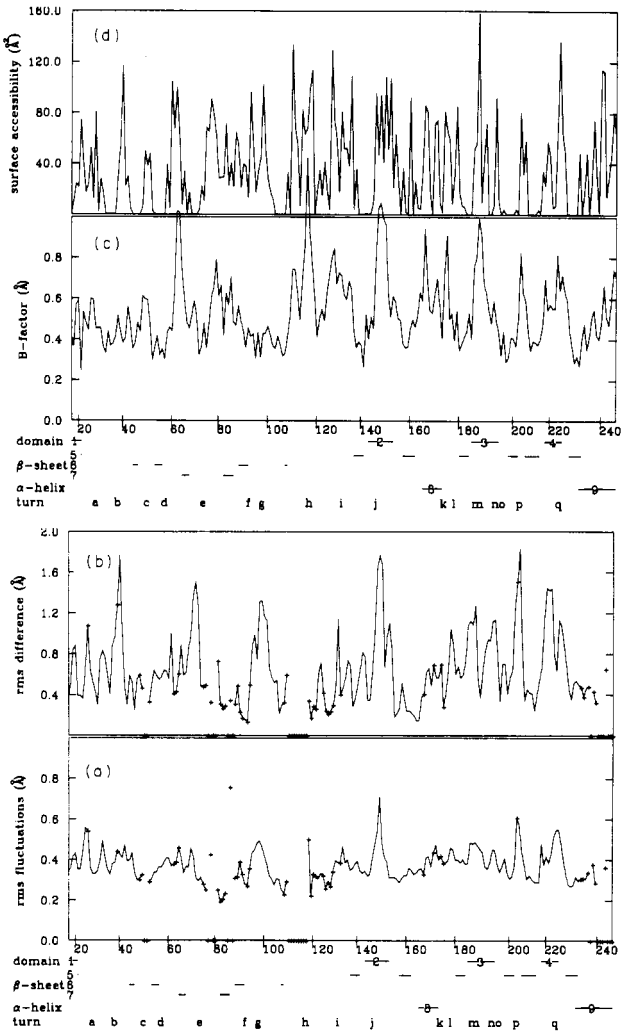

FIGURE 4: (a) rms fluctuations of the TrMD1 average structure, (b) rms difference between the TrMD1 average structure and the X-ray structure, (c) X-ray B factors of trypsin converted to rms fluctuations, and (d) surface accessibility of the X-ray structure. The properties have been averaged over main-chain atoms (C, N, C^{α}) except for the surface accessibilities, where the sum over all atoms of a residue was computed. Residues with one or more atoms in the buffer region are indicated by a +. The values for excluded region residues have been set to zero. The labeling is according to Table I.

RESULTS

The results of the various SBMD simulations are discussed in the following sections. The β-sheets, α-helices, and β-turns in trypsin have been labeled to simplify references to them (cf. Figures 4 and 6); the labeling scheme is given in Table I.

Features of the SBMD Simulation of Native Trypsin (TrMD1). The C^{α} backbone of the average TrMD1 structure is compared to the C^{α} backbone of the X-ray structure of trypsin in Figure 3, and the rms deviations between the two structures averaged over main-chain atoms are shown in Figure 4b. The deviations between the average TrMD1 structure and the X-ray structure are 1.33 and 0.77 Å for unconstrained atoms (i.e., atoms in the reaction region) and constrained atoms, respectively; for the continued simulation TrMD2 the deviations are 1.42 and 0.79 Å relative to the X-ray structure compared to 0.34 and 0.36 Å relative to the TrMD1 structure. These differences indicate that the average structures, though not necessarily the fluctuations (see below), of TrMD1 and TrMD2 have converged. There are only five small regions with deviations from the X-ray structure larger than 1.5 Å (Figure 4b). The list of hydrogen bonds for the activation domain and surroundings in Table II shows that most hydrogen bonds of the X-ray structure are reproduced in the molecular dynamics average structure TrMD1. Results of a simulation of trypsin under vacuum (not shown) yielded much larger deviations;

Table II: Comparison of Hydrogen Bonds in the X-Ray Structure of Trypsin and in Molecular Dynamics Average Structures TrMD1 and Tr(−16,17)MD[a]

hydrogen bond donor	hydrogen bond acceptor	distance[b] (Å) Tr	TrMD1	Tr(−16,17)-MD
Activation Domain (Internal)[c]				
Ile-16 (N)	Gly-142 (O)		2.6	
Ile-16 (N)	Asn-143 (O)	3.0	3.6	
Val-17 (N)	Asp-189 (O)	2.8	2.9	
Gly-18 (N)	Thr-144 (O)		3.8	
Asn-143 (N)	Gln-192 (O)	2.9	3.1	3.2
Asn-143 (ND2)	Ser-147 (O)			3.0
Asn-143 (ND2)	Gly-148 (O)	3.1	2.8	
Thr-144 (N)	Ser-150 (O)	3.0	2.9	3.0
Thr-144 (OG1)	Ser-150 (O)	2.9	2.8	
Lys-145 (N)	Asn-143 (OD1)	3.1	3.0	3.3
Lys-145 (NZ)	Thr-144 (O)	3.9		
Ser-147 (OG)	Ser-146 (O)	3.4		
Ser-150 (N)	Asn-143 (OD1)	2.8	3.2	2.9
Gly-187 (N)	Tyr-184 (O)	2.9	4.0	3.6
Gly-188A (N)	Ala-221A (O)	2.9		
Lys-188 (N)	Gly-187 (O)	3.2	2.9	2.8
Asp-189 (N)	Val-17 (O)	3.1	3.2	
Ser-190 (N)	Asp-189 (OD2)	2.8	3.3	3.3
Ser-190 (OG)	Asp-189 (OD2)	3.7		
Gln-192 (NE2)	Tyr-151 (OH)	3.6		
Gln-192 (N)	Gly-219 (O)			3.0
Ala-221A (N)	Asp-189 (OD1)	3.0	3.0	3.1
Gln-221 (NE2)	Ser-146 (O)	3.8		
Lys-222 (NZ)	Gln-186 (O)		2.7	2.7
Asn-223 (N)	Leu-185 (O)	2.7	3.0	3.0
Activation Domain ↔ Surroundings				
Ile-16 (N)	Asp-194 (OD1)	2.7	2.7	
Ile-16 (N)	Asp-194 (OD2)	3.5	2.9	
His-40 (NE2)	Gly-193 (O)	3.0		
Gly-142 (N)	Gly-140 (O)	3.8		4.0
Gly-142 (N)	Asp-194 (OD2)	2.8	3.0	
Gly-184A (N)	Pro-161 (O)	3.0	3.0	2.9
Tyr-184 (OH)	Lys-159 (O)	2.8	2.8	
Ser-190 (N)	Tyr-228 (OH)	3.9	2.8	2.8
Cys-191 (N)	Asp-194 (OD1)	2.8	2.9	3.9
Asp-194 (N)	Cys-191 (O)	3.0	3.1	3.3
Asp-194 (N)	Gln-192 (O)	3.7	3.7	
Ser-217 (N)	Tyr-172 (OH)	3.2		
Ser-217 (OG)	Tyr-172 (OH)		3.1	2.8
Lys-224 (N)	Gln-221 (O)	3.1	3.5	3.8
Lys-224 (N)	Lys-222 (O)		3.5	3.0
Tyr-228 (OH)	Asp-189 (OD2)	4.0		

[a] Criteria for the existence of a hydrogen bond: donor–acceptor distance <4.0 Å; donor–hydrogen–acceptor angle <60°. [b] Between the donor and the acceptor atoms. [c] Activation domain defined as residues 16–19, 142–152, 184A–193, and 216–223.

parts of the activation domain drifted by more than 6 Å. This suggests that the solvent environment stabilizes the exposed activation domain, at least on the time scale of the molecular dynamics simulation.

Residues that were partially constrained or excluded in the SBMD buffer region are marked by a cross in all figures. The excluded regions of the SBMD simulation are between turns c and d, between turns e and f, and around turn h and the C-terminal α-helix. As the constrained or excluded residues are far from the activation domain, the influence of the stochastic boundary conditions on the properties of the activation domain is negligible.

The fluctuations of the main-chain atoms around their average positions in TrMD1 are shown in Figure 4a; the values are averaged over main-chain atoms for each residue. In parts c and d of Figure 4 the temperature factors and the surface accessibilities (Lee & Richards, 1971) of the X-ray structure are shown. Relative to the rest of the molecule, the activation domain exhibits an increased mobility in both the X-ray

Table III: Root Mean Square Fluctuations[a]

region	ident	structure X-ray	TrMD1	TrMD2	Tr(−16,17)-MD
activation domain	1	0.50	0.39	0.48	0.76
activation domain	2	0.76	0.44	0.54	0.44
activation domain	3	0.67	0.43	0.41	0.38
activation domain	4	0.64	0.47	0.46	0.40
β-sheet	5	0.40	0.34	0.35	0.34
β-sheet	6	0.38	0.34	0.30	0.29
β-sheet	7	0.58	0.40	0.33	0.34
α-helix	8	0.63	0.40	0.36	0.40
α-helix	9	0.40	0.30	0.32	0.30
turns		0.59	0.43	0.40	0.40

[a] Values (Å) averaged over unconstrained main-chain atoms.

structure and the TrMD1 average structure, particularly for segments 2 and 4; for segment 3 the X-ray results show similar behavior to segments 2 and 4 while the TrMD1 simulation has smaller fluctuations (see Table III). In the simulation the fluctuations of segment 3 are of the same order of magnitude as parts of the trypsin structure not involved in α-helices or β-sheets (e.g., the segment between turns g and h). The activation domain contains no α-helical or β-strand structural elements (see Table I); i.e., it consists of large segments of random-coil residues with a number of well-defined turns (turn j in segment 2, m and n in segment 3, q in segment 4). β-Sheets generally show smaller temperature factors as well as rms fluctuations with the exception of the solvent-exposed and relatively short β-sheet 7, which has rather high temperature factors (see Table III). In the TrMD1 simulation, β-sheet 7 is partially constrained but still exhibits increased rms fluctuations for the unconstrained atoms. The two α-helical regions 8 and 9 show somewhat larger temperature factors than the β-sheets, particularly for the C-terminal α-helix 9. Both α-helices are more than 22 Å away from the center of the activation domain and were only partially included in the simulation; therefore, the α-helices do not show increased rms fluctuations.

Most regions with large experimental temperature factors are located in the vicinity of β-turns, e.g., turns c, i, h, k, and p. The turns are near the surface of the molecule as can be assessed from the surface accessibilities (Figure 4d). Turns such as a, b, d, g, i, j, l, n, m, o, p, q (see Figure 4a) that are not too close to excluded regions also exhibit larger than average fluctuations in TrMD1.

The magnitudes of the rms fluctuations for the flexible regions are generally smaller in the MD simulation than those observed in the X-ray structure (Figure 4a,c). This is probably due to the short 10-ps sampling period over which the average fluctuations were computed. However, for the perturbation studies presented in this paper, where corresponding simulations are being compared, it is not essential to have fully converged fluctuations.

Effect of Replacing the Ile-16 and Val-17 Residues by Water. The effect of replacing the Ile-16 and Val-17 residues by water molecules is illustrated in Figure 5, which shows the C^{α} backbone of the molecular dynamics average structures TrMD1 and Tr(−16,17)MD before and after removal of the dipeptide; Figure 6b gives the rms difference between the two structures on a per residue basis.

The conformational changes between TrMD1 and Tr(−16,17)MD are confined to the activation domain, the N-terminal region, and the turns a, b, d, f, g, and p. These conformational changes are 1–2 Å in magnitude and are

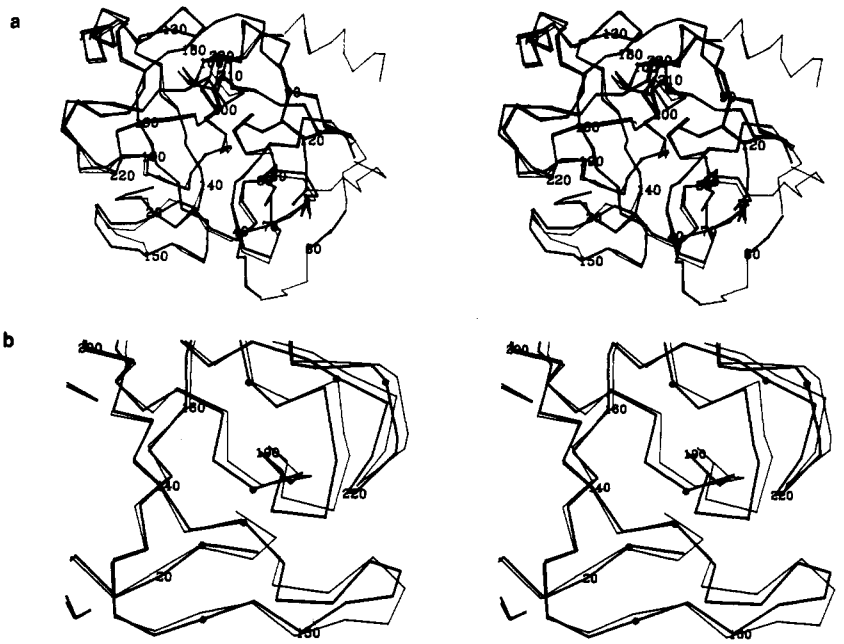

FIGURE 5: Comparison of the C^{α} backbone of the molecular dynamics average structure of TrMD1 (thick lines) and the average molecular dynamics structure of Tr(−16,17)MD (thin lines): (a) same view as in Figures 1 and 2; (b) close-up view of the activation domain.

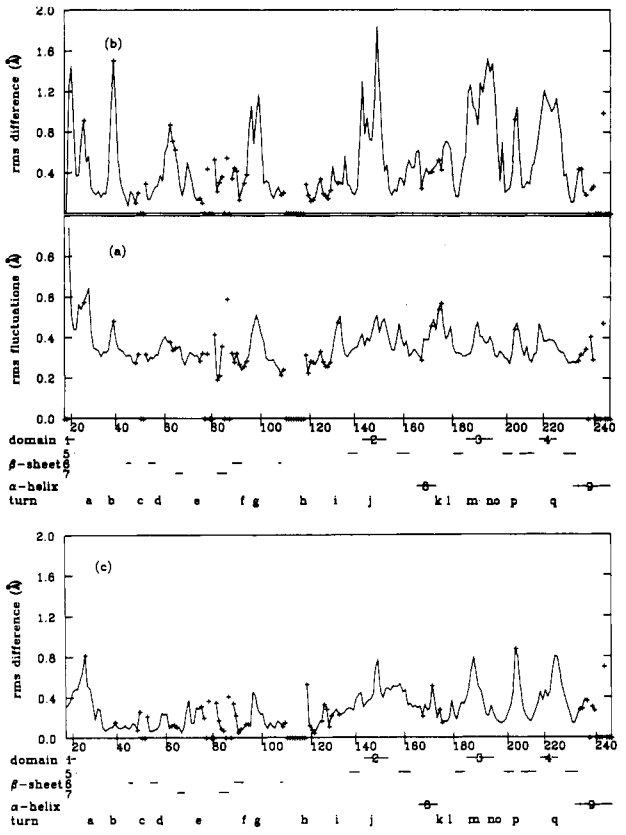

FIGURE 6: (a) rms fluctuations of the Tr(−16,17)MD average structure, (b) rms difference between the Tr(−16,17)MD and the TrMD1 average structures, and (c) rms difference between the TrMD2 average structure and the TrMD1 average structure. Labeling is similar to that in Figure 3.

significantly larger than the rms fluctuations in TrMD1 (see Figure 4b) or Tr(−16,17)MD itself (see Figure 6a). Thus, these deviations are not due to a random fluctuation of the system. To examine the possibility that the conformational change is simply a continuing drifting motion already present in the TrMD1 run, Figure 6c shows the difference of the molecular dynamics average structures between TrMD1 and TrMD2, the 10-ps continuation of TrMD1. There are displacements in parts of the activation domain and in turns a and p. However, the changes in Figure 6c are significantly smaller than those in Figure 6b, and they affect only a few residues in the activation domain (e.g., for region 2 only Ser-146, Ser-147, Gly-148, and Thr-149 instead of Gly-140 through Val-154); by contrast, the conformational change in the pertubed structure (Figure 6b) affects all residues of the activation domain. Thus, the observed conformational changes of the activation domain appear to be induced by the replacement of residues Ile-16 and Val-17 with water molecules. Of particular interest is the fact that the conformational change in the activation domain found in the simulation is confined to the regions that have been shown to be disordered in the X-ray structure of trypsinogen (Huber & Bode, 1978). Since most of the protein was included in the simulation and no constraints were applied in the vicinity of the activation domain, this correspondence is not an artifact of the simulation method.

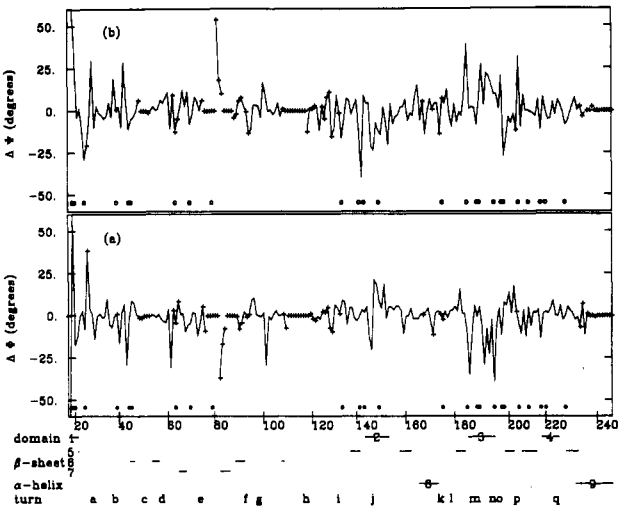

FIGURE 7: (a) Difference in ϕ angles and (b) difference in ψ angles between the average structures of TrMD1 and Tr(−16,17)MD. The labeling is similar to that in Figure 3. Glycine residues are marked by o.

The conformational change is a long-range effect since some residues in the activation domain that are affected by the

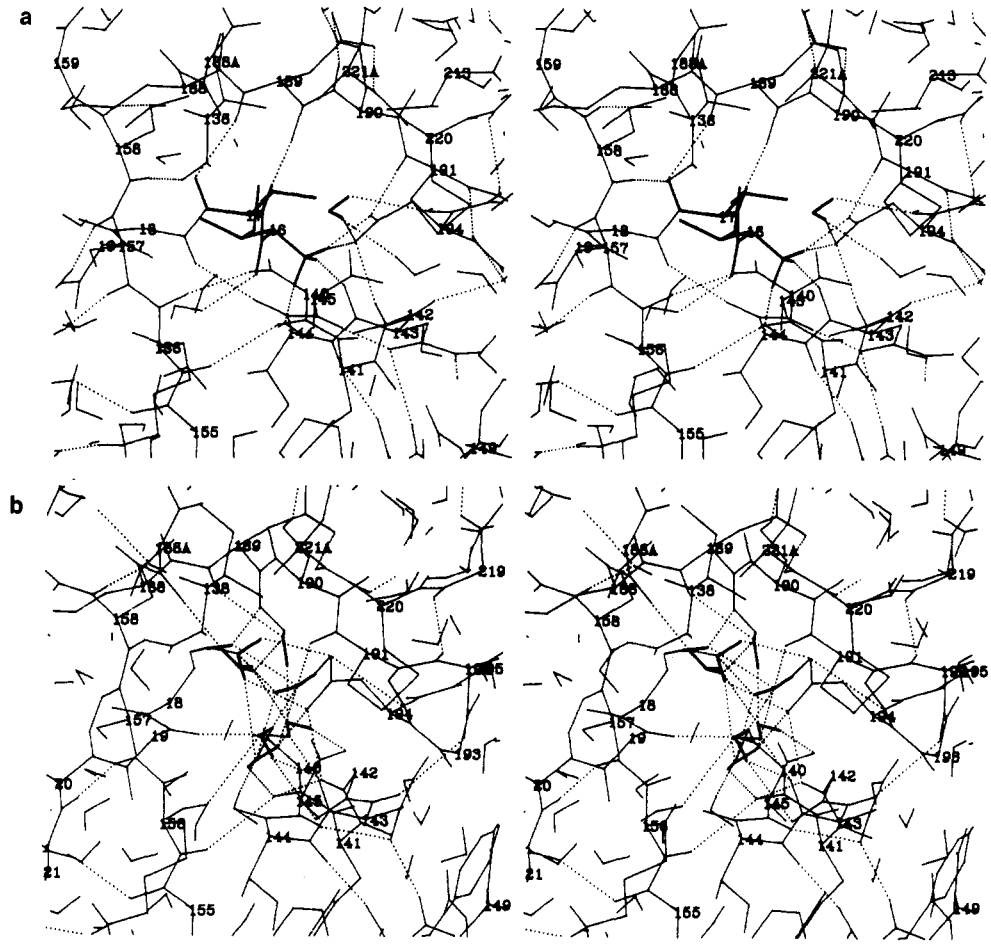

FIGURE 8: Stereoview of the N-terminal binding pocket in (a) TrMD1 and (b) Tr(−16,17)MD. The Ile-16 and Val-17 residues as well as the waters in the binding pocket are marked with thick lines. Hydrogen bonds are indicated between protein atoms as well as between pocket waters and surroundings if the following criteria are met: the heavy donor–acceptor distance is less than 4.0 Å and the donor–hydrogen acceptor angle is less than 60°.

removal of the Ile-16 and Val-17 residues are more than 15 Å from the N-terminus. In particular, residues in segment 4 do not interact directly with Ile-16 and Val-17, yet they exhibit large conformational changes (cf. Figure 6b). It is likely that the perturbation is propagated through segment 3, which is in contact with segment 4 (see Figure 5b). The structural change is terminated at the junctions between the activation domain and β-sheet 5 (Figure 6b).

By removal of the two N-terminal residues, the interactions between the N-terminus and the activation domain have been interrupted. In particular, the hydrogen bonds Ile-16···Asp-194/Gly-142/Asn-143, Val-117···Asp-189, and Gly-18···Thr-144 (see Table II) are lost, and the N-terminal arm (residues Gly-18 through Cys-22) is free to drift somewhat, as it probably does in trypsinogen. The observed motion extends up the start of β-sheet 5 near Tyr-20. Most hydrogen bonds between the activation domain and its surroundings (Table II) remain intact in Tr(−16,17)MD. However, the hydrogen bond Tyr-184···Lys-159 is lost, and all hydrogen bonds to Asp-194 are either broken or weakened (Asp-194···Gln-192, Gly-142···Asp-194, Cys-191···Asp-194). Asp-194 is in a somewhat different conformation in Tr(−16,17)ME than in TrMD1 (Figure 8), but it does not rotate to form a hydrogen bond to His-40, as observed in the trypsinogen X-ray structure (Fehlhammer et al., 1977). Since the simulation was limited to 30 ps, it is unlikely to reproduce such a large conformational change, particularly if there is a significant activation barrier.

The motion of turns a, b, d, f, g, and p in the dynamics simulation (Figure 6b) cannot be explained by direct interactions with the activation domain as they are respectively 10, 9, 5, 12, 6, and 9 Å from the nearest atom of any residue of the activation domain. Presumably the displacements of these turns arise from the flexibility of these surface regions (see above). In some cases (e.g., turns a and p) similar drifts occur in the simulation TrMD2 relative to TrMD1. It is likely that the same argument applies to turns b, d, f, and g, but longer simulations are needed in order to confirm this suggestion (Elber & Karplus, 1987).

To further characterize the conformational change of the activation domain, the main-chain dihedral angle (ϕ, ψ) differences between TrMD1 and Tr(−16,17)MD are shown in Figure 7a,b. They clearly reflect the rms differences in Figure 6b: i.e., regions of large rms differences also contain a few residues with large ϕ and/or ψ differences and vice versa. The largest changes in ϕ or ψ dihedral angles occur in Gly residues (they are marked with o in Figure 7a,7b), e.g., Gly-23 in turn a, Gly-142 and Gly-148 in domain 2, Gly-184A, Gly-187, Gly-188A, Gly-193, Gly-196, and Gly-197 around domain 3, Gly-203 in turn p, and Gly-216 in domain 4. Glycine residues exhibit changes in ϕ or ψ angles that are larger than the changes in these angles for the residues that surround them; i.e., the glycine residues correspond to local maxima or minima in the ϕ or ψ difference curves. The preferred mobility of the protein main chain near glycine residues is not surprising as the absence of a side chain leads to a lower torsional barrier for the rotation around ϕ and ψ bonds. The results suggest that the glycine residues act as hinges for the conformational

change of the activation domain segments with the remainder moving as a fairly rigid units (Huber & Bode, 1978).

Water Network in the N-Terminal Binding Pocket of Tr(−16,17)MD. Parts a and b of Figure 8 show a close-up view of the N-terminal binding pocket of the average structures in TrMD1 and Tr(−16,17)MD, respectively. The binding pocket is defined by segments Asp-189 through Asp-194 and Gly-142 through Thr-144. The Ile-16 and Val-17 residues form a number of hydrogen bonds to the segments of the activation domain (Table II and Figure 8a), as well as hydrogen bonds to water molecules near residues Lys-156 and Thr-144 (Figure 8a); these water molecules are on the surface of the protein and are close to positions of ordered water molecules seen in the trypsin X-ray structure. One water molecule is present in the binding pocket in TrMD1 (it is marked with thick lines in Figure 8a); this water is not seen in the X-ray structure. Residues Ile-16 and Val-17 are replaced by eight water molecules (they will be referred to as the "pocket" waters), including the water in TrMD1, as can be seen by comparing parts a and b in Figure 8. In the X-ray structure of the trypsinogen–PTI complex (Bode et al., 1976) six water molecules are located in approximately the same region. Two of them are within hydrogen-bonding distance of Asp-194 and Asn-143, and five of them appear to form hydrogen bonds among themselves. The pocket waters in the simulation form a hydrogen-bonding network with the same residues with which the N-terminus was forming hydrogen bonds, in particular with Asp-194, Asn-143, and Gly-142. The pocket waters do not exchange with other water molecules during the 10-ps simulation; they oscillate around their average positions, with the rms fluctuations between 0.51 and 0.78 Å. It is these waters that "mimic" the N-terminus in the Tr(−16,17)MD system. However, they are expected to have considerably greater flexibility than the normal N-terminus, since they can diffuse to accommodate changes in protein structure and thus permit the observed displacements to occur.

Conclusions

To explore the nature of the trypsinogen to trypsin transition, we have performed stochastic boundary molecular dynamics simulations for the solvated trypsin molecule in its native form and in a state where the Ile-16 and Val-17 N-terminal residues were replaced by water molecules. The latter simulation introduces a perturbation that models one of the differences between trypsin and trypsinogen.

The simulation of native trypsin is generally in good agreement with the X-ray structure in terms of the average positions of the atoms and the fluctuations relative to the average positions. A corresponding simulation in the absence of solvent showed much larger structural deviations (unpublished calculations).

Replacement of the Ile-16 and Val-17 N-terminal residues induces a conformational transition of the activation domain. This conformational transition involves almost exactly the same range of residues that is disordered in trypsinogen. The presence of glycines in the activation domain appears to facilitate the conformational transition, as indicated by the large main-chain ϕ and ψ angle differences in these residues. The water molecules that replace the N-terminal Ile-16 and Val-17 mimic the missing residues by forming a hydrogen-bonded network with the protein. An estimate of the binding enthalpy of the N-terminus (Brünger and Karplus, unpublished results) suggests that the solvent interactions have a strong influence on the binding.

Future investigations of the degree of flexibility of the TrMD1 and Tr(−16,17) structures should be made by using more drastic perturbations than in the present study, e.g., by pulling away parts of the activation domain, by changing the conformation of Asp-194, or by heating the system. Stochastic and activated dynamics would be useful for simulating the disorder transition (McCammon et al., 1980). Also, for the N-terminal residues and the Ile-Val dipeptide (Bode, 1979), an estimate of the free energy of binding would be of interest.

Mutagenesis and X-ray structure determinations for T4 phage lysozyme (Grutter & Matthews, 1982) and theoretical predictions followed by X-ray determinations of a mutant of haemagglutinin (Shih et al., 1985; Knossow et al., 1984) have suggested that only localized conformational changes occur on single-site substitutions if a stable protein results. The present results show that the entire activation domain in trypsin is sensitive to a modification of the N-terminus. This indicates that there can be regions in proteins stable to the replacement of individual amino acids and other regions where larger scale changes are induced; e.g., a portion of the protein structure is destabilized relative to the random-coil form by replacing or removing one or more amino acids. The activation domain in trypsin seems to be an example of the latter type that was presumably engineered by evolution to make possible the zymogen to active enzyme transition. Thus, trypsinogen activation is an excellent system for analysis by combined site-specific mutagenesis and structure determinations. The gene of trypsin has been cloned and expressed, and several mutants have been synthesized recently (Craik et al., 1985). Tests of hypotheses concerning the importance of specific residues in the activation domain transition should now be possible. It would be of great interest to substitute some of the key glycine residues or Asp-194 in trypsin and trypsinogen; also, removal of the Ile-16 and Val-17 N-terminal residues in trypsin could provide further insight into the nature of the transition.

Acknowledgments

We are grateful to W. Bode for discussions of the activation domain problem. We thank C. L. Brooks III and G. A. Petsko for useful suggestions.

References

Ansari, A., Berendzen, J., Bowne, S. F., Frauenfelder, H., Iben, I. E. T., Saucke, T. B., Shyamsunder, E., & Young, R. D. (1985) *Proc. Natl. Acad. Sci. U.S.A. 82*, 5000–5004.

Bennett, W. S., & Huber, R. (1985) *CRC Crit. Rev. Biochem. 15*, 291–354.

Blow, D. M. (1976) *Acc. Chem. Res. 9*, 145–152.

Bode, W. (1979) *J. Mol. Biol. 127*, 357–374.

Bode, W., & Schwager, P. (1975) *J. Mol. Biol. 98*, 693–717.

Bode, W., & Huber, R. (1976) *FEBS Lett. 68*, 231–236.

Bode, W., Fehlhammer, H., & Huber, R. (1976) *J. Mol. Biol. 106*, 325–335.

Bode, W., Schwager, P., & Huber, R. (1978) *J. Mol. Biol. 118*, 99–112.

Brooks, B. R., Bruccoleri, R. E., Olafson, B. D., States, D. J., Swaminathan, S., & Karplus, M. (1983) *J. Comput. Chem. 4*, 187–217.

Brooks, C. L., & Karplus, M. (1983) *J. Chem. Phys. 79*, 6312–6325.

Brooks, C. L., Brünger, A., & Karplus, M. (1985a) *Biopolymers 24*, 843–865.

Brooks, C. L., Pettitt, B. M., & Karplus, M. (1985b) *J. Chem. Phys. 83*, 5897–5908.

Bruccoleri, R. E., & Karplus, M. (1986) *J. Comput. Phys.* (in press).

Brünger, A. T., & Karplus, M. (1987) (submitted for publication).

Brünger, A. T., Brooks, C. L., & Karplus, M. (1984) *Chem. Phys. Lett. 105*, 495–500.
Brünger, A. T., Brooks, C. L., & Karplus, M. (1985) *Proc. Natl. Acad. Sci. U.S.A. 82*, 8458–8462.
Butz, T., Lerf, A., & Huber, R. (1982) *Phys. Rev. Lett. 48*, 890–893.
Chambers, J. L., & Stroud, R. M. (1977) Brookhaven Protein Data Bank, file 3PTP.
Chou, P. Y., & Fasman, G. D. (1978) *Adv. Enzymol. Relat. Areas Mol. Biol. 47*, 45–148.
Cohen, G. H., Silverton, E. W., & Davies, D. R. (1981) *J. Mol. Biol. 148*, 449–479.
Craik, C. S., Largman, C., Fletcher, T., Roczniak, S., Barr, P. J., Fletterick, R., & Rutter, W. J. (1985) *Science (Washington, D.C.) 228*, 291–297.
Elber, R., & Karplus, M. (1987) *Science (Washington, D.C.) 235*, 318–321.
Fehlhammer, H., Bode, W., & Huber, R. (1977) *J. Mol. Biol. 111*, 415–438.
Grutter, M., & Matthews, B. (1982) *J. Mol. Biol. 154*, 525–535.
Huber, R., & Bode, W. (1978) *Acc. Chem. Res. 11*, 114–122.
Huber, R., & Bennett, W. S. (1983) *Biopolymers 22*, 261–279.
Huber, R., Kukla, D., Bode, W., Schwager, P., Bartels, K., Deisenhofer, J., & Steigemann, W. (1974) *J. Mol. Biol. 89*, 73–101.
Jones, T. A. (1982) in *Computational Crystallography* (Sayre, D., Ed.) pp 303–317, Clarendon, Oxford.
Jorgensen, W. L., Chandrasekhar, J., & Madura, J. D. (1983) *J. Chem. Phys. 79*, 927–935.
Keil, B. (1971) *Enzymes (3rd Ed.) 3*, 249–275.
Knossow, M., Daniels, R. S., Douglas, A. R., Skehel, J. J., & Wiley, D. C. (1984) *Nature (London) 311*, 678–680.
Kossiakoff, A. A., Chambers, J. L., Lois, M. K., & Stroud, R. M. (1977) *Biochemistry 16*, 654–664.
Lee, B., & Richards, F. M. (1971) *J. Mol. Biol. 55*, 379–400.
McCammon, J. A., & Karplus, M. (1983) *Annu. Rev. Biochem. 53*, 263–300.
McCammon, J. A., Gelin, B. R., & Karplus, M. (1977) *Nature (London) 267*, 585–590.
McCammon, J. A., Northrup, S. H., Karplus, M., & Levy, R. M. (1980) *Biopolymers 19*, 2033–2045.
Nadler, W., Brünger, A. T., Schulten, K., & Karplus, M. (1986) *Biopolymers* (submitted for publication).
Pflugrath, J. W., Saper, M. A., & Quiocho, F. A. (1984) in *Methods and Applications in Crystallographic Computing* (Hall, S., & Ashida, T., Eds.) pp 404–407, Clarendon, Oxford.
Powell, M. J. D. (1977) *Mathematical Programming 12*, 241–254.
Ryckaert, J. P., Cicotti, G., & Berendsen, H. J. C. (1977) *J. Comput. Phys. 23*, 327–337.
Shih, H. H.-L., Brady, J., & Karplus, M. (1985) *Proc. Natl. Acad. Sci. U.S.A. 82*, 1697–1700.
Sigler, P. B., Blow, D. M., Matthews, B. W., & Henderson, R. (1968) *J. Mol. Biol. 35*, 143–164.
Verlet, L. (1967) *Phys. Rev. 159*, 98–105.
Walter, J., Steigemann, W., Singh, T. P., Bartunik, H., Bode, W., & Huber, R. (1982) *Acta Crystallogr., Sect. B: Struct. Crystallogr. Cryst. Chem. B38*, 1462–1472.
Wang, C., & McCammon, J. A. (1986) *Isr. J. Chem.* (in press).
Wang, D., Bode, W., & Huber, R. (1985) *J. Mol. Biol. 185*, 595–624.